

DEVELOPMENT OF A DESIGN BASIS TORNADO

and

STRUCTURAL DESIGN CRITERIA

for

LAWRENCE LIVERMORE LABORATORY'S
SITE 300, CALIFORNIA

by

James R. McDonald, P.E.
Joseph E. Minor, P.E.
Kishor C. Mehta, P.E.

FINAL REPORT

prepared for
STRUCTURAL MECHANICS GROUP
Nuclear Test Engineering Division
LAWRENCE LIVERMORE LABORATORY
University of California
Livermore, California

P.O. 5062405

MASTER

November 1975

NOTICE
This report was prepared as an account of work sponsored by the United States Government. Neither the United States nor the United States Energy Research and Development Administration, nor any of their employees, makes any warranty, expressed or implied, or assumes any legal liability or responsibility for the accuracy, completeness or usefulness of any information, apparatus, product or process disclosed, or represents that its use would not infringe privately owned rights.

McDONALD, MEHTA and MINOR
Consulting Engineers
Lubbock, Texas

DISTRIBUTION OF THIS DOCUMENT IS UNLIMITED

FOREWORD

The development of recommendations for a design basis tornado and structural design criteria for use in evaluating critical facilities at the Site 300 was conducted under Purchase Order No. 5062405 with Lawrence Livermore Laboratory, University of California. Mr. Robert C. Murray of the Structural Mechanics Group, LLL, served as the technical representative for monitoring the project. Dr. James R. McDonald represented the consulting firm of McDonald, Mehta and Minor as principal investigator. Dr. Richard E. Peterson, a meteorologist, also contributed to the technical effort.

TABLE OF CONTENTS

	<u>Page</u>
FOREWORD	1
LIST OF TABLES	iii
LIST OF ILLUSTRATIONS	iv
I. INTRODUCTION	1
II. DEVELOPMENT OF A DESIGN BASIS TORNADO	2
A. Meteorological Considerations	2
B. Historical Records for California	3
C. Tornado Records	4
D. Tornado and Extreme Wind Risk Model	16
E. Tornado and Extreme Wind Parameters at Site 300	16
F. Relationship of Proposed Design Criteria to Other Available Criteria	21
III. GUIDELINES FOR DESIGN LOADS	24
A. General	24
B. Wind Induced Loads	24
C. Design for Missiles	27
D. Design Example	38
APPENDIX A	54
APPENDIX B	55
LIST OF REFERENCES	58

LIST OF TABLES

<u>Table</u>		<u>Page</u>
I	Tornado Occurrences and Intensities in Four State Area Surrounding Site 300 (1959-1973)	6
II	Tornado Occurrences in 3-Degree Region Surrounding Site 300 (1959-1973)	6
III	Computations: Tornadic Wind Occurrence Probability Distribution	12
IV	Probability Distributions for Site 300, California . .	16
V	Recommended Wind Parameters	19
VI	Velocity Pressure Coefficient, K_2	25
VII	Effective Mass of Target During Impact	35
VIII	Recommended Ductility Ratios	37
IX	Numerical Solution to Equations of Motion	52

LIST OF ILLUSTRATIONS

<u>Figure</u>		<u>Page</u>
1	Tornado Occurrence in 3-Degree Region Surrounding Site 300	7
2	Number of Tornadoes Exceeding Threshold Windspeeds	10
3	Recommended Tornado and Extreme Wind Risk Models for Site 300	17
4	Values of Penetration Coefficient K_p for Reinforced Concrete	33
5	Idealized Resistance-Displacement Function for Ductile Materials	33
6	Plan View of Example Structure	39
7	Structural Response of a Reinforced Concrete Wall	45
8	Reinforced Concrete Wall Cross Section	46
9	Force-Time Function and Resistance Function	46
B1	Fisher-Tippett Type II Probability for Site 300	57

I. INTRODUCTION

The purpose of this document is to prescribe criteria and to provide guidance for professional personnel who are involved with the evaluation of existing buildings and facilities at Site 300 near Livermore, California. It is intended that this document be used in the evaluation of critical facilities to resist the possible effects of extreme winds and tornadoes. The document contains two major sections: (1) development of parameters for the effects of tornadoes and extreme winds and (2) guidelines for evaluation and design of structures.

The report presents a summary of the investigations conducted and contains discussions of the techniques used for arriving at the combined tornado and extreme wind risk model. The guidelines for structural design methods for calculating pressure distributions on walls and roofs of structures and methods for accommodating impact loads from missiles are also presented.

II. DEVELOPMENT OF A DESIGN BASIS TORNADO

A. Meteorological Considerations

Climatic conditions in California range from subtropical to alpine. A diverse blending of simpler climate types results from two major weather controls acting over this region of great latitude extent and range of altitudes. In California, however, there is not usually the coincidence of factors which, in the Midwest, are precursors of tornadic activity: a strong low-level flow of warm, moist air; a dry middle-level current; surmounted by a more westerly strong jet stream.

In the summer months, the central coastal regions of California are dominated by a northward extension of the North Pacific subtropical high. Depressions are usually deterred from impinging along the California coast. Furthermore, the persistent anticyclonic subsidence in combination with the upwelling of cold water along the coast produces a quite stable and widespread inversion. Convective activity is usually suppressed; most stations experience a rainless summer with storminess confined to the period from October through May (Trewartha, 1961)*.

Moisture flow from the west migrates southward during the winter with the southward shift of the subtropical high and the Pacific cyclone belt. The greatest inflow, however, lies north of 40°N lat. (Rasmussen, 1967). At the surface, stations receive their greatest

* References may be found in the alphabetically arranged List of References by referring first to author name and then to publication date.

precipitation amounts in December through February. However, the rainfall and storminess are rapidly attenuated inland across successive ranges of greater and lesser elevations.

Occasional strong thunderstorms may develop with the destabilization accompanying the passage of a cold upper level trough at any time of year. In winter, post-frontal instability showers can develop in the cool air overlying the then relatively warm ocean. In either case, tornadic activity may arise; however, the intensity would only rarely be sufficient to overcome the topographic weakening of the storms.

B. Historical Records for California

The meteorological records testify to the temperateness of the climate. California encompasses a large area; nevertheless, the number of recorded tornadoes has been relatively small (NSSFC, 1974). Early tornado incidence maps (Court, 1970) did not designate tornado-prone regions within California until 1930 (Day, 1930). At that time a small frequency of occurrence was noted for the Southern California and San Francisco Bay regions. This pattern has recurred on most subsequent depictions with a gradual extension of observed activity into the San Joaquin Valley (e.g., Pautz, 1969).

Analyzing United States records for 1880-1942, Showalter and Fulks (1943) found that in California (based on a total of 15 tornado days) a slight maximum of annual activity occurs in March and April. More recent compilations for 1950-1971 (Smith and Mirabella, 1972) bear out this earlier conclusion; for a total of 38 tornado days, April and May lead with 9 and 8 days, respectively, followed by a relative maximum in November with 6 days.

For the period 1918-1960, Critchfield (1960) found a statewide frequency of about 0.5 per year. Since that time, the annual frequency has inched upward: from almost 1 (USWB, 1962); to 2 (USWB, 1965); to past 3 (Pautz, 1969).

The tornado hazard then in California is not great; however, as Californians spread over all parts of their state, more of the weaker storms will be detected. Among those will be funnels and tornadoes in the Livermore area; its location inland along with the surrounding hilliness will serve, though, to diminish the likelihood of very strong or long-lasting activity.

Based on approximately 20 years of records, the mean dewpoint temperature for Sacramento, Fresno, San Francisco and Eureka is 46°F (adjusted to sea level). The highest monthly average at Sacramento is 53°F (U.S. Department of Commerce 1968). The average dewpoint temperatures are at least marginal for thunderstorm activity. Charts presented by Dodd (1965) show the standard deviation in addition to the mean monthly values.

C. Tornado Records

The State of California has experienced relatively few tornadoes when compared with states east of the Rocky Mountains. Only 17 events were listed in the period 1892 through 1949. Forty-eight cases were recorded in the 22 year period from 1950-1971 (Smith and Mirabella, 1972). Because of the general absence of conditions favorable for tornado formation and because of the records, damage from tornadoes in the State of California does not appear to be a significant threat.

Tornadoes occurring during the period 1959-1973 in California and the surrounding states of Arizona, Nevada and Utah are summarized in Table I. Tornadoes occurring within a 3-degree square surrounding Site 300 during the same period are summarized in Table II. Tornado occurrence locations and relative windspeed intensities, presented using Fujita's F-Scale (Fujita, 1971), are included in Figure 1. See Appendix A for explanation of Fujita Scale.

D. Tornado and Extreme Wind Risk Model

The above reviews of the published literature and reviews of both published and unpublished tornado occurrence records indicate that tornadic vortices are uncommon in California due to the absence of energy sources and strong wind shears needed to spawn severe tornadoes.

Design standards that are incorporated into building codes do not normally include the effects of tornadoes in their wind load criteria. Some tornado risk models ignore the presence of nontornadic extreme winds. The literature reviews and data evaluations suggest that design basis extreme windspeeds and associated tornado effects for Site 300 should be developed from available tornado records used in combination with extreme wind data available elsewhere in the literature. Furthermore, the design basis extreme winds and tornado effects should be developed on a probabilistic basis which relates extreme windspeeds with a probability of occurrence.

1. Methodology for Developing the Tornado Portion of the Risk Model

Since tornado intensities are expressed in terms of Fujita-Pearson Scales (FPP-Scales), the tornado risk model was developed on

TABLE I
TORNADO OCCURRENCES AND INTENSITIES IN FOUR STATE AREA
SURROUNDING SITE 300 (1959-1973)

[SOURCES: NOAA (Storm Data), NSSFC 1974]

<u>State</u>	<u>F0</u>	<u>F1</u>	<u>F2</u>	<u>F3</u>	<u>TOTAL</u>
Arizona	23	20	18	4	65
California	18	11	4	-	33
Nevada	8	3	1	-	12
Utah	12	9	5	-	26
<u>Total</u>	<u>61</u>	<u>43</u>	<u>28</u>	<u>4</u>	<u>136</u>

* Refer to Appendix A for discussion of Fujita's Intensity Scale.

TABLE II
TORNADO OCCURRENCES IN 3-DEGREE REGION SURROUNDING SITE 300 (1959-1973)
[SOURCES: NOAA (Storm Data), NSSFC 1974]

<u>State</u>	<u>F0</u>	<u>F1</u>	<u>F2</u>	<u>F3</u>	<u>TOTAL</u>
California	10	3	-	-	13

CALIFORNIA

NEVADA

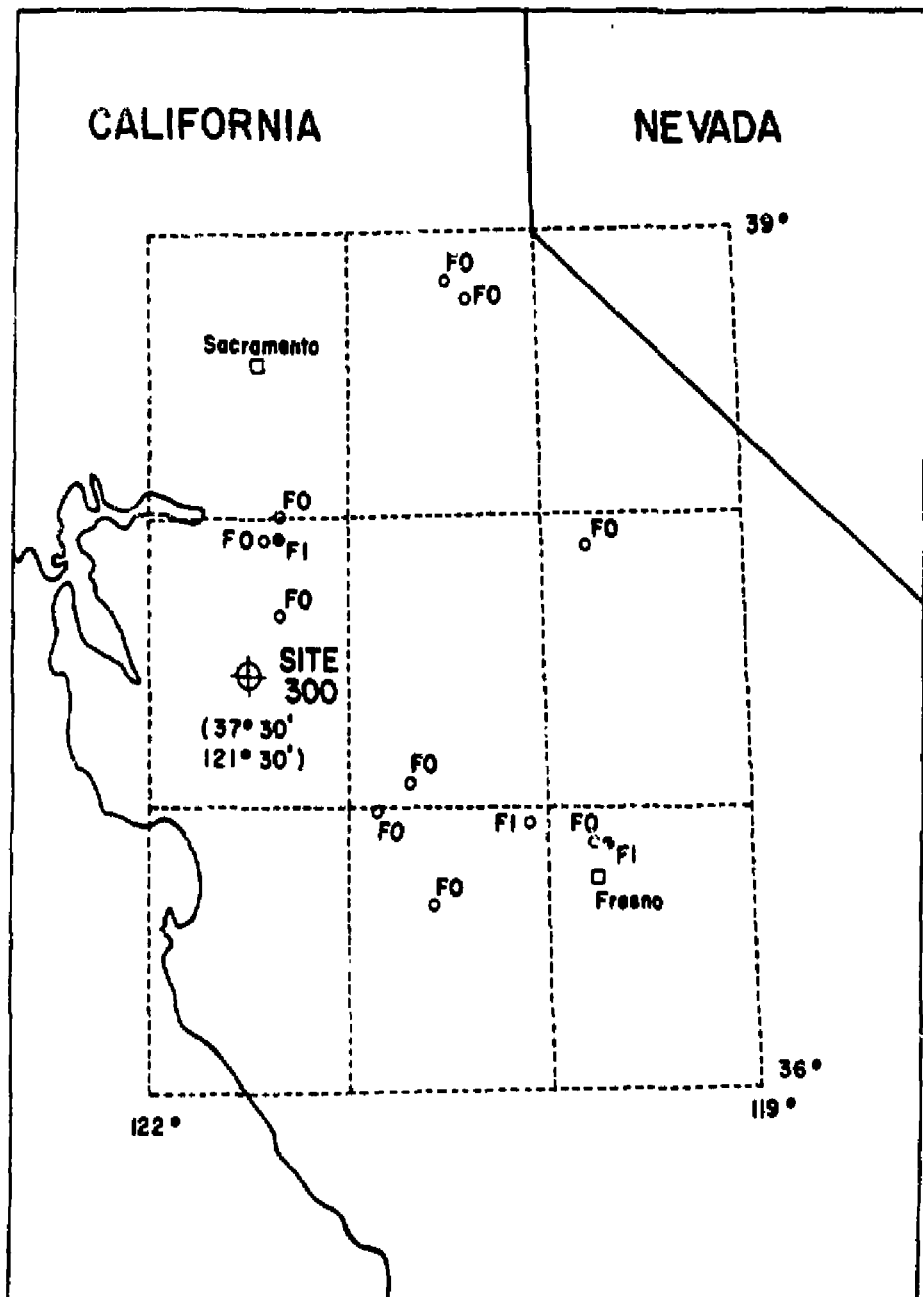


FIGURE 1 TORNADO OCCURRENCE IN 3-DEGREE REGION SURROUNDING SITE 300

this basis. Four basic steps are involved:

- (1) Determination of the mean area of tornado damage based upon tornadoes which occurred in the four state area surrounding Site 300.
- (2) Determination of the average number of tornadoes per year for each F-Scale intensity classification in a 3-degree square surrounding Site 300.
- (3) Calculation of the probability of occurrence of tornadoes exceeding a threshold windspeed within a 3-degree square area.
- (4) Determination of the probability that windspeeds in tornadoes will exceed the threshold value.

a. Mean Damage Area

There was an insufficient number of tornado occurrences in the 3-degree square around Site 300 to make a statistically reliable prediction of the mean damage areas for each F-Scale classification of tornadoes. Although this procedure has been employed in other tornado risk model developments (McDonald 1974, 1974a), a different procedure was employed in the Site 300 study. In the modified procedure a larger geographical region (consisting of the State of Nevada, and parts of the States of Utah, Arizona, and California) was used to determine a single average damage area for all tornadoes occurring in the four state area. The NSSFC tape (NSSFC 1974) gives a Pearson path length (P_L) and path width (P_W) for most tornadoes in the four state region for the three year period 1971-1973. From the P_L and P_W ratings the damage area in square miles was determined for these tornadoes using the median length and width in each Pearson scale classification. The mean damage area for tornadoes in the four state area was then computed from these data.

b. Average Number of Tornadoes Per Year

The number of tornadoes in the 3-degree square was obtained from the master list discussed above. These data are presented in Table II and in Figure 1. F-Scale ratings were assigned by the authors on the basis of damage descriptions from Storm Data (NOAA), if they were not provided by the NSSFC computer tape. In some instances the descriptions in Storm Data were vague or non-existent. A conservative F-Scale rating was assigned in these cases. Once these ratings had been made, the average number of tornadoes exceeding any threshold windspeed was determined for the region. The number of tornadoes exceeding the wind-speed represented by each F-Scale rating was plotted or shown in Figure 2. A regression analysis was performed to obtain the number of tornadoes exceeding any threshold velocity. With this information, the average number of tornadoes per year exceeding the threshold velocity was found.

c. Probability of Occurrence

By having the mean damage path area and the average rate of occurrence per year for any arbitrary threshold windspeed, the probability of occurrence of tornadoes having any arbitrary threshold wind-speed could be determined by using the relationship

$$P_i = \frac{Y_i \bar{A}}{A}, \quad (1)$$

where:

Y_i is the average rate of tornado occurrence per year for the threshold windspeed V_i (tornadoes/year, from Figure 2)

\bar{A} is the mean tornado damage path area in sq mi

A is the total area within the 3-degree square surrounding Site 300 (sq mi).

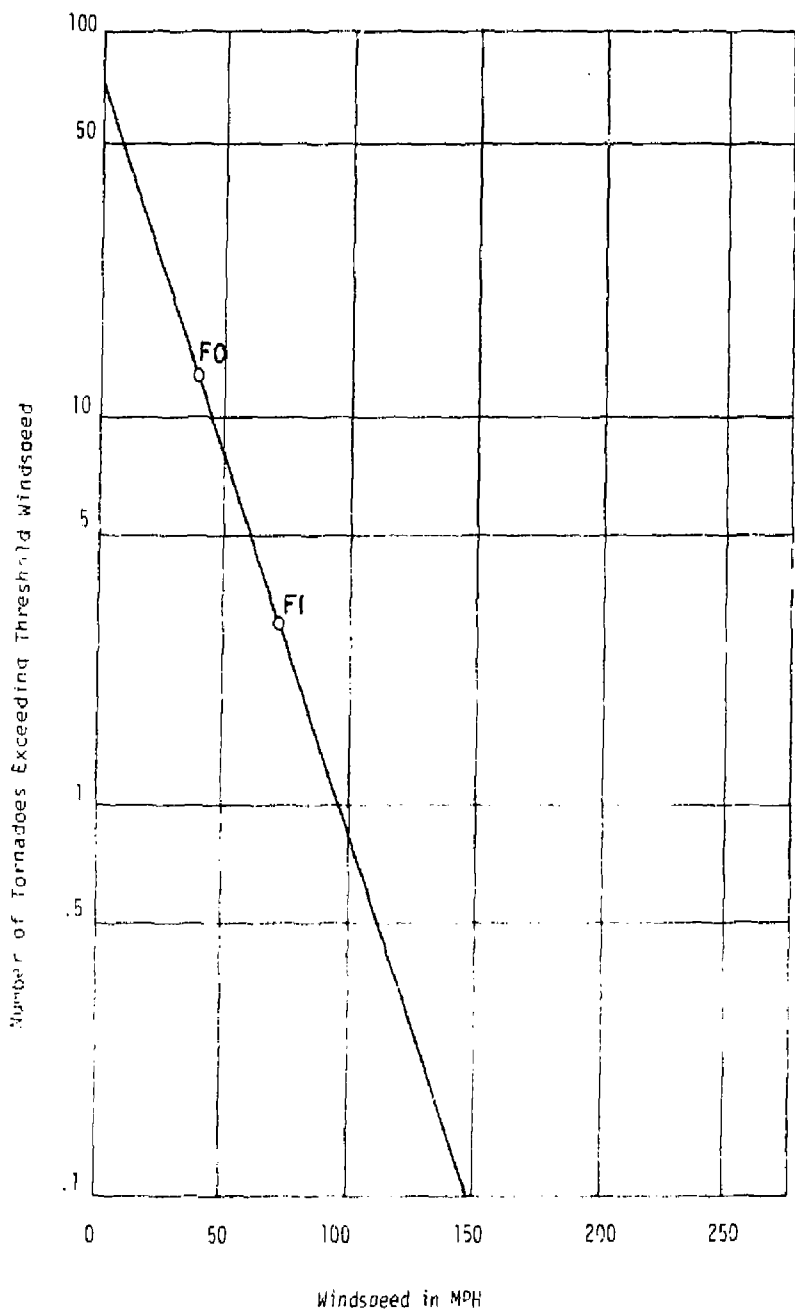


FIGURE 2. NUMBER OF TORNADOES EXCEEDING THRESHOLD WINDSPEEDS

d. Probability of Windspeeds Exceeding a Threshold Value

The probability of winds exceeding a windspeed corresponding to a specific threshold value, V_i , is obtained by taking the cumulative sum of the probabilities of the threshold values higher than the one under consideration.

$$P_E = \sum_{i=1}^n P_i \quad (2)$$

where n is related to the largest threshold velocity considered.

Table III contains a summary of the results of the study to determine the tornado occurrence probability distribution.

2. Methodology for Determining the Straight Wind Portion of the Risk Model

The work of Thom (1968) is used to evaluate the probability of straight winds exceeding any threshold value of windspeed. Thom's data specifically excludes tornadoes from the data set.

a. Windspeed Records

The probability distributions for straight winds developed by Thom are based on records of extreme annual fastest mile windspeeds. The records cover a 21 year period and were accumulated at 150 locations in the contiguous United States.

b. Straight Windspeed Distribution

Because winds are bounded at zero and are generally thought of as being unlimited above zero, Thom selected the Fisher-Tippet Type II distribution for straight winds. The data set of annual extreme fastest mile windspeeds for each weather station, after being corrected for elevation and terrain roughness, was fitted to the Fisher-Tippet Type II probability distribution. The expression for the cumulative

TABLE III
COMPUTATIONS: TORNADIC WIND OCCURRENCE PROBABILITY DISTRIBUTION

	Threshold Windspeed (mph)						
	50	100	150	200	250	300	350
Number of tornadoes exceeding threshold windspeed	8.3	0.90	0.097	0.011	0.0012	0.00012	0.000014
Number of tornadoes in the threshold interval	7.4	0.81	0.087	0.0095	0.0010	0.00011	0.000014
Number of tornadoes per year, γ_i	5.0×10^{-1}	5.4×10^{-2}	5.8×10^{-3}	6.3×10^{-4}	6.8×10^{-6}	7.4×10^{-6}	9.0×10^{-7}
Mean damage area, \bar{A} (sq mi)	0.39	0.39	0.39	0.39	0.39	0.39	0.39
Geographic area, A (sq mi)	34,100	34,100	34,100	34,100	34,100	34,100	34,100
Probability of occurrence of threshold value, P_i (per year)	5.6×10^{-6}	6.1×10^{-7}	6.6×10^{-8}	7.2×10^{-9}	7.7×10^{-10}	8.4×10^{-11}	1.0×10^{-11}
Probability of exceeding threshold value, P_E (per year)	6.3×10^{-6}	6.8×10^{-7}	7.4×10^{-8}	8.0×10^{-9}	8.7×10^{-10}	9.4×10^{-11}	1.0×10^{-11}

probability per year of not exceeding a windspeed value V is

$$F(V) = \exp [-(V/\beta)^{-\gamma}] \quad (3)$$

where β and γ are chosen to fit the annual extreme fastest mile wind data set for the geographical location under consideration. Thom constructed a special probability paper (See Fig. B1) on which the Fisher-Tippett Type II distribution plots as a straight line. A simple logarithmic transformation of Equation 3 puts it in the form

$$y = a + bx, \quad (4)$$

where a and b are parameters that define the straight line relationship. A regression analysis then yields values of the parameters a and b for the best fit straight line through the data points. The a and b terms in Equation 3 are related to the values of a and b . The distributions were fitted to 150 stations to obtain data for the wind probability maps of the United States for mean recurrence intervals of 2, 10, 25, 50 and 100 years (Thom, 1968). The mean recurrence interval is given by

$$T = \frac{1}{1 - F(V)} \quad (5)$$

A transformation involving logarithms of the extreme windspeeds can be made to obtain the Fisher-Tippett Type I model. This is the model that was actually used by Thom (1968) in his latest work. This mathematical model is also known as the Frechet distribution function.

C. Windspeed Distribution for Site 300

Figure B1 in the Appendix shows information on windspeed distributions for three cities (where data were available) in the general

area around Site 300. These distributions are based on extreme fastest mile windspeed data obtained from Environmental Data Service, Asheville, North Carolina. The distributions are Fisher-Tippett Type II. The five points shown on Figure B1 represent windspeeds obtained from the mean recurrence interval maps of Thom (1968) for Site 300. A regression analysis was performed using these five points to obtain a windspeed distribution applicable to Site 300. Examination of this distribution shows that it predicts unreasonably high windspeeds, especially at the 10^{-4} and 10^{-6} occurrence per year levels of risk. Since Thom did some smoothing of the isotach lines, the distribution at Site 300 appears to be influenced by the windspeed distribution for Sacramento. The distribution for Sacramento is unlike the distributions obtained for other locations. The slope of the probability distribution line (Fig. B1) is much flatter for Sacramento than for the other two California cities. The slope is also much flatter when compared with other locations in Nevada, Kansas, Tennessee and Texas. Although there is a difference in windspeed values for a given risk level the distribution lines for Fresno and Red Bluff are essentially parallel. If only the lower four points from the Thom maps are used, the distribution obtained is also essentially parallel to the ones for Fresno and Red Bluff. This distribution predicts windspeeds of 110 and 185 mph for the 10^{-4} and 10^{-6} risk levels. It is the authors' opinion that this distribution is consistent with conditions at Site 300 and that designs based on these values will be consistent with the goals of protecting public health and safety.

Although Thom's data is corrected for terrain roughness and elevation of wind measuring instruments, locations near the mouths of valleys

and on the lee side of mountain ranges must be given special consideration. Because of the channeling effects observed along Corral Hollow at Site 300, some increase in windspeeds above those predicted by the Fisher-Tippett distribution can be expected. The technical literature is sparse on the quantification of channeling effects, and measurements at the site for comparison with nearby sites are not readily available. To account for the channeling effect, it is recommended that the windspeeds obtained from the Fisher-Tippett distributions (Fig. B1) be increased by 10 per cent. Thus the 110 and 185 mph values cited above should be increased to 121 and 203 mph, respectively, to account for channeling.

The extrapolation of the straight wind curve into the 200 mph or greater regime must be discussed in terms of confidence limits. There is always some uncertainty as to the line of best fit through the data points. Thus any value quoted from the wind model is the expected value. The expected value is expected to be exceeded half the time and not be exceeded half the time. Therefore, there is a band of confidence (or band of uncertainty) associated with any statement from the model. If more data points are used (additional years of records) the band of confidence narrows. However, since the expected value line is extrapolated beyond the data points, as is done in this study, the band of confidence becomes extremely wide.

3. The Risk Model: Combined Effects of Straight Winds and Tornadoes

The combined probability distribution of both tornadoes and straight winds is approximately equal to the sum of the two distributions. The probability of the union of two events is approximately equal to the sum of the probabilities of the individual events, if the probability of their intersection is small (Neville and Kennedy, 1966). Values for

the straight wind (Fisher-Tippett Type II) distribution, the tornado distribution and the combined distribution are given in Table IV, and are plotted in Figure 3. It is clear that the probability of tornado occurrence is so small that it has no effect on the combined distribution, which allows for the possibility of tornadoes or extreme winds at the site.

TABLE IV
PROBABILITY DISTRIBUTIONS FOR SITE 300, CALIFORNIA
(STRAIGHT WINDS, TORNADOES, AND COMBINED)

<u>Windspeed</u>	<u>Straight Wind Distribution</u>	<u>Tornado Distribution</u>	<u>Combined Distribution</u>
50	9.4×10^{-2}	6.3×10^{-6}	9.4×10^{-2}
100	2.3×10^{-4}	6.8×10^{-7}	2.3×10^{-4}
150	6.4×10^{-6}	7.4×10^{-8}	6.4×10^{-6}
200	5.2×10^{-7}	8.0×10^{-9}	5.2×10^{-7}
250	7.3×10^{-8}	8.7×10^{-10}	7.3×10^{-8}
300	1.5×10^{-8}	9.4×10^{-11}	1.5×10^{-8}
350	3.8×10^{-9}	1.0×10^{-11}	3.8×10^{-9}

E. Tornado and Extreme Wind Parameters at Site 300

Determinations of specific tornado and extreme wind parameters for any specific geographic location must involve: (1) the tornado and extreme wind risk model and (2) a definition of the acceptable level of risk for structures and facilities under consideration. The

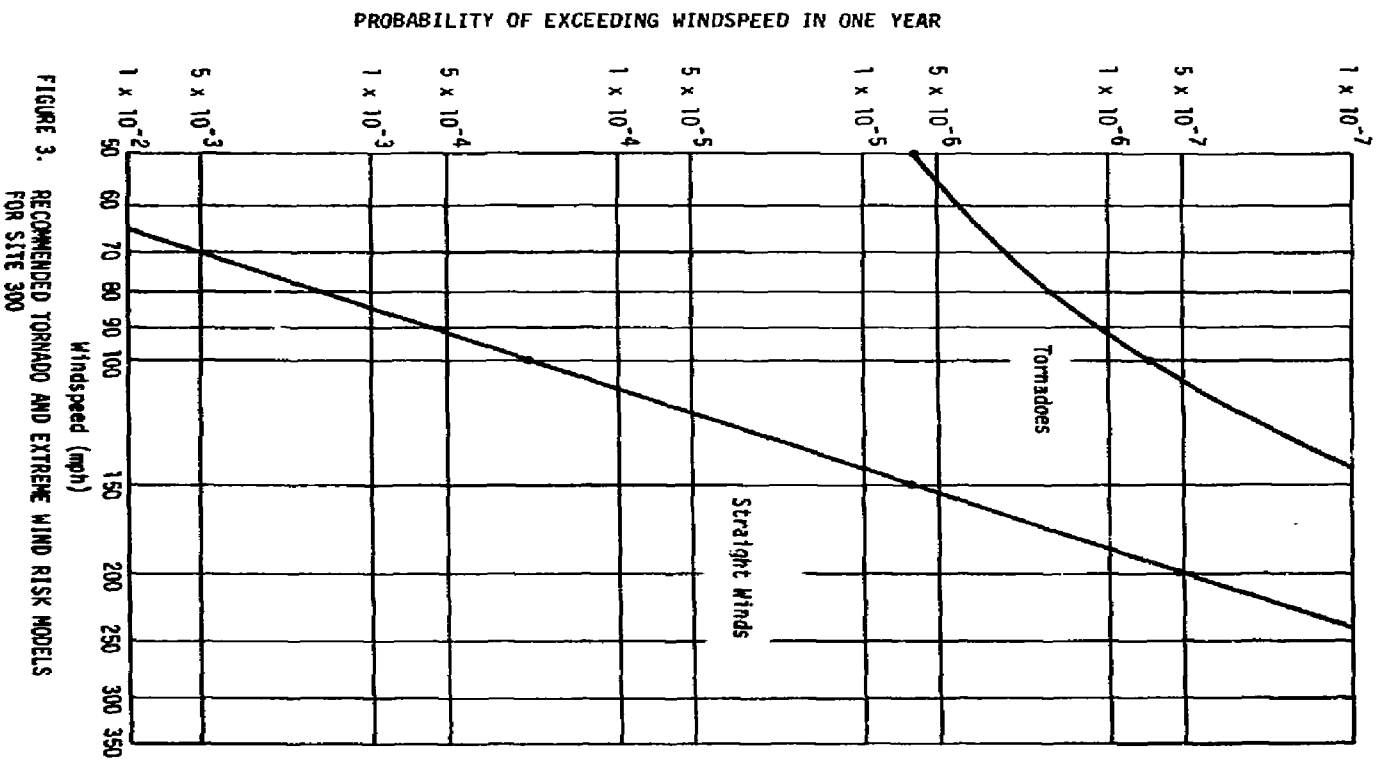


FIGURE 3. RECOMMENDED TORNADO AND EXTREME WIND RISK MODELS FOR SITE 300

risk model involves the curves developed for Site 300 presented in Figure 3. The latter, level of risk definition, is defined by the responsible contractor organization acting in coordination with the Energy Research and Development Agency (ERDA). In the case of Site 300, the responsible contractor organization (Lawrence Livermore Laboratory) has advanced two levels of risk for evaluating existing facilities at Site 300. The levels of risk are stated as 1×10^{-4} and 1×10^{-6} probability of occurrence per year for design tornado and extreme wind parameters.

With the risk model and acceptable levels of risk having been defined, it remains only to develop a listing of specific tornado and extreme wind parameters. Reference to Figure 3 reveals that the maximum design windspeeds associated with the 1×10^{-4} and 1×10^{-6} levels of risk are 110 mph and 185 mph respectively. Note that the tornado windspeeds associated with these levels of risk are negligible compared with those for straight winds. This conclusion confirms the more general observations made in the meteorological discussion (Section II), i.e., available data suggest that severe tornadoes are not a significant threat in the area surrounding Site 300. Furthermore, this interpretation of the risk model suggests that extreme straight winds should be the governing design parameter as the straight wind probability curve dominates the combined tornado-straight wind curve (Ref. Fig. 3).

The above interpretations of the risk model (for the levels of risk selected) produce the recommended wind parameters advanced in Table V. For the selected level of risk, the straight wind parameters dominate the design parameters. Atmospheric pressure change is thus not a significant design parameter. The design parameters reflect the

TABLE V
RECOMMENDED WIND PARAMETERS -- SITE 300

RISK: 1×10^{-6} occurrence/year

Maximum Windspeed*	185 mph
Effective Velocity Pressure	106 psf
Missiles: 4 x 12, 12 ft long timber, 139 lbs, area 41.7 in. ²	90 mph (horizontal) 60 mph (vertical)
400 lb automobile	25 mph (tumbling on ground)

RISK: 1×10^{-4} occurrence/year

Maximum Windspeed*	110 mph
Effective Velocity Pressure	38 psf
Missile: 2 x 4, 12 ft long timber, 20 lb, area 5.9 in. ²	70 mph (horizontal)

*The design basis tornadoes associated with the 1×10^{-4} and 1×10^{-6} levels of risk will pose no threat to critical facilities designed to withstand the maximum (straight) wind. Hence no parameters for translational, rotational, tangential, radial, or vertical windspeeds, for atmospheric pressure change, or for tornado-generated missiles are advanced. The effective velocity pressure includes a 10 per cent increase in windspeed because of the channeling effect of the wind at the site.

effects of straight wind and the missiles which can be produced by these windspeed values.

The design basis missiles advanced in Table V were developed by considering (1) the character of structures at Site 300 which might, upon failure, contribute to the missile environment and (2) the trajectory predicted by injecting the missiles into an analogous windfield. A computer program developed at Texas Tech was used to determine the expected accelerations, velocities and trajectories of potential missiles injected into the windfield. The following assumptions are made in the computer program:

- (1) Aerodynamic drag coefficients of 1.0 and 1.2 are used for cylindrical and parallelepipeds respectively
- (2) The missiles assume a nontumbling mode with their largest surface area normal to the relative wind velocity vector
- (3) A tornado windfield patterned after the Dallas Tornado of 1957 (Hoecker, 1960) is used.

Assumptions 2 and 3 are both conservative. The missiles are likely to tumble because of turbulence. Missiles are more likely to be picked up by tornadic winds than by straight winds.

Four different missiles were considered with the 185 mph windspeed (1×10^{-6} occurrence/year):

- (1) Timber plant 4 x 12, 12 ft long at 139 lbs
- (2) Steel pipe, Schedule 40, 3 in. dia., 10 ft long at 76 lbs
- (3) Utility pole, 13.5 in. dia., 35 ft long at 1490 lbs
- (4) Automobile, 4000 lbs.

Results from the computer program showed that only the 4 x 12 timber plank would be sustained in the assumed windfield. The 3 in. dia. pipe and the utility pole were thus ruled out as potential missiles. The

automobile is not sustained in the windfield, but could roll or tumble along the ground. Therefore, it was included as a plausible missile. This decision agrees with observations of windstorm damage in the field (McDonald 1974, 1974a).

None of the four missiles would be suspended in the 110 mph windfield (1×10^{-4} occurrence/year). As a minimum criterion, the 2 x 4 x 12 ft long timber at 70 mph (horizontal) is recommended.

F. Relationship of Proposed Design Criteria to Other Available Criteria

Design criteria developed by Smith and Mirabella (1972) and that proposed in AEC Regulatory Guide 1.76 (AEC 1974) are available and are applicable to the geographic region containing Site 300. In this section the proposed criteria is discussed in light of these two previous studies.

1. AEC Regulatory Guide 1.76

The AEC Regulatory Guide 1.76 (AEC 1974) suggests criteria for tornado resistant design in Zone II with the following parameters:

Maximum Horizontal Windspeed 300 mph

Total Pressure Drop 2.25 psi

These criteria are based on a level of risk of 1×10^{-7} , which is considered appropriate for nuclear power plant sites. The technical basis for the Regulatory Guide criteria is contained in WASH-1300 (Markee, Beckerly and Sanders, 1974). The technique described in the WASH-1300 report was applied to a 3-degree square region surrounding Site 300. For a level of risk corresponding to 10^{-6} the technique predicts a maximum expected tornado windspeed of 210 mph. This compares with a value of 92 mph determined in the present study for the same level of risk.

There are two major differences in the approaches used for determining the tornado risk models:

- (1) In calculating the probability of a strike the WASH-1300 report procedure employs a mean tornado damage area of 2.82 sq mi. This differs considerably from the 0.39 sq mi area determined from tornado records of the four state area surrounding Site 300. Smith and Mirabella (1972) found that the mean damage area of California tornadoes (1951-1971) was only 0.11 sq mi.
- (2) The authors of the WASH-1300 report base their intensity-occurrence relationship on a region (Zone III) that is considerably larger than the 3-degree square surrounding Site 300.

In general, the study published in the WASH-1300 report represents an attempt to regionalize tornado criteria for the entire United States. The recommendations are admittedly "interim" criteria. The results of the present study represent detailed investigations into both the meteorology of the site and the statistics of the tornado records. The proposed criteria based on the present study are consistent with the spirit of the WASH-1300 report, and they represent a comparable level of safety based on the best information available at the site.

2. Study by Smith and Mirabella

In a study performed in 1972 Smith and Mirabella concluded that the maximum windspeed in California tornadoes is not expected to exceed 200 mph (rotational plus translational speed). These conclusions were supported by a study of the characteristics of California tornadoes and statements by Dr. Edwin Kessler, Director, National Severe Storms Laboratory and Dr. Ted Fujita of the University of Chicago. Both are recognized experts in the field of tornado climatology.

Although a probability of tornado strike was calculated by Smith and Mirabella (3.4×10^{-6} occurrences per year), no attempt was made to

develop a tornado risk model. The criteria recommended by them represents a consensus of upper bound tornadic windspeeds. The present study attempts to refine the estimates and represents advances in the state-of-the-art in tornado parameter prediction. The criteria recommended in this study is consistent with the work of Smith and Mirabella. What the present work does show is that tornadoes do not pose a significant threat of damage to critical structures at the site. The probability of straight wind occurrences is significantly greater at all levels of risk.

III. GUIDELINES FOR DESIGN LOADS

A. General

This section addresses the translation of tornado and extreme wind parameters from Table V into recommended pressure distributions and missile impact loads on walls and roofs. Because the most significant design parameter is a straight wind, the approach to developing wind induced pressure distributions follows, as a guide, the procedures advanced in the American National Standards Institute Standard, ANSI A58.1-1972 (ANSI 1972). The approaches used in developing missile impact resistant designs follow previously advanced procedures formulated by the nuclear power industry.

Since these guidelines are to be used for evaluating the structural integrity of critical facilities at Site 300, it will be assumed in presenting design pressures and missile impact loads that:

- (1) the pressures and loads given will be treated as ultimate loads, and
- (2) structures will be analyzed and designed by plastic or ultimate strength methods using these ultimate loads.

B. Wind Induced Loads

1. Effective Velocity Pressure

An effective velocity pressure $q = 106$ psf shall be used as the basic value. This effective velocity pressure is applicable to building heights of 30 ft. or less. For velocity pressures at heights greater than 30 ft. the 1/7 power law shall be applied. The effective velocity pressure at height z is given by

$$q_z = 106 K_z, \quad (7)$$

where values of K_z are given in Table VI. Buildings and structures exceeding 200 ft. in height will require special engineering attention which is beyond the scope of these design guidelines.

TABLE VI
VELOCITY PRESSURE COEFFICIENT, K_z

Height Above Ground (ft)	K_z^*
≤ 30	1.0
50	1.16
100	1.41
150	1.58
200	1.72

$$*K_z = \left(\frac{z}{30}\right)^{\frac{2}{7}}$$

Critical structures are to be analyzed and designed by plastic or ultimate strength procedures; hence, the effective velocity for critical structures represents an ultimate loading condition.

2. Design Wind Pressures

Critical structures which by definition must maintain structural integrity at design windspeed should be designed for external pressures

only. (i.e., Do not include atmospheric pressure change associated with tornado.) Design wind pressures are equal to the product of the effective velocity pressure q and appropriate pressure coefficients. External pressure coefficients C_p are used with the effective velocity pressure to obtain design pressures for components according to the equation:

$$p = q C_p \quad (8)$$

Care must be exercised in using Equation 8 as the sign of the design pressure p is very important. A positive value for design pressure ($+p$) means inward acting pressure, and a negative value for design pressure ($-p$) means outward acting pressure. The signs for C_p , referenced in ANSI (1972), are self correcting, and appropriate signs should be used in Equation 8 to obtain proper signs for the design pressure p . Building components such as walls and roofs should be designed for maximum inward acting pressures and maximum outward acting pressures. The pressure coefficients presented in this document are taken from the American National Standards Institute, Building Code Requirements for Minimum Design Loads in Building and Other Structures (ANSI 58.1-1972).

External pressure coefficients C_p depend upon the type of components being considered and the building geometry.

Walls: External pressure coefficients C_p for walls are given in ANSI A58.1, Table 7, p. 19. The windward wall experiences a positive design pressure ($+p$) while the leeward and side walls experience negative design pressure ($-p$). The pressure coefficients for the leeward wall depend on the ratio of height to horizontal dimension. At all corners

a local external pressure coefficient of -2.0 shall be used over a small area to account for localized turbulence. These relatively high local pressures are assumed to act on strips of width $0.1w$, where w is the least width of the building. These local pressures are not used in combination with other pressures on the walls in the determination of overall loads.

Roofs: Flat, arched, and sloped roofs with winds acting parallel to roof surfaces have negative external pressure coefficients. The values of the coefficients depend on the dimensions of the structure. For buildings with a ratio of wall height to least width of less than 2.5, an external pressure coefficient of -0.7 shall be used for the roof, and the computed pressure shall be assumed uniform over the entire roof area. For buildings in which the height to width ratio is 2.5 or greater, a value of -0.8 shall be used for the entire roof area.

Arched roofs have both positive and negative external pressure coefficients for wind perpendicular to the axis of the arch. The roof area is divided into three parts: windward quarter, center half, and leeward quarter. The magnitude and sign of the pressure coefficients depend upon the rise to span ratio. Coefficients for arched roofs are given in ANSI ASB.1, Table 8, p. 19.

Gabled roofs require a pressure coefficient of -0.7 on the leeward slope for wind perpendicular to the gable. The values and signs of external pressure coefficients on the windward slope depend on the slope of the roof and on the ratio of wall height to least width dimension. Values are given in ANSI ASB.1, Table 9, p. 19.

At ridges, eaves and 90-degree corners of roofs, local peak external pressures shall be computed using the pressure coefficients given in ANSI ASB.1, Table 10, p. 20. These local pressures shall not be used in combination with other roof pressures.

C. Design for Missiles

Critical structures shall be designed to resist the missiles specified in Table V. The missiles are assumed to strike normal to the wall or roof surface with the minimum cross sectional area (on-end). In addition, at critical locations the structure should be checked for damage because of collapse of columns, walls, or rigid

frames resulting from the impact of a tumbling automobile.

1. Penetration Formulas

The penetration of a missile represents a local effect. The prediction of damage includes an estimation of the depth of penetration, the minimum thickness required to prevent perforation and the minimum thickness to preclude spalling. As used in this document, perforation means that the missile passes through the wall or roof target, penetration means that the missile embeds itself in the target.

a. Reinforced Concrete Target

The Modified Petry Formula is recommended for reinforced concrete targets. The depth to which a rigid missile will penetrate a reinforced concrete target of infinite thickness is estimated by the formula:

$$D = 12 K_p A_p \log_{10} \left(1 + \frac{V_s^2}{215,000} \right) \quad (9)$$

where

D = Depth of penetration (in.)

K_p = Penetration coefficients for reinforced concrete (see Fig. 4 for values)

A_p = Impact pressure (psf); Missile weight (lbs)/contact area (ft^2)

V_s = Missile strike velocity (ft/sec).

When the wall has a finite thickness, the depth of penetration is

$$D_1 = \left[1 + e^{-4(\frac{T}{D} - 2)} \right] D \quad (10)$$

where

T = Thickness of the slab (in.)

e = Base of Natural logarithms

When the wall thickness, T , is $2D$, the penetration $D_p = 2D$ and the wall is just perforated. In order to prevent spalling, the thickness of the wall shall be a minimum of $3D$.

b. Steel Target

The Ballistic Research Laboratory (BRL) Formula is recommended for penetration and perforation of steel targets. The steel plate thickness (in.) that will just be perforated is

$$T = \frac{\left(\frac{M_m V^2}{2}\right)^{2/3}}{672 d_m} \quad (11)$$

where

M_m = Mass of the missile (slugs)

V = Velocity of the missile (ft/sec)

d_m = Diameter of the missile (in.)

For an irregularly shaped missile an equivalent diameter is used. The equivalent diameter is the diameter of a circle with an area equal to the circumscribed contact, or projected frontal area of the noncircular missile. The thickness to prevent perforation should be taken as

$$T_p = 1.25T \quad (12)$$

The residual velocity (V_r , in ft/sec) after perforation is given by the following equation:

$$V_r = [V_s^2 - \frac{1.12 \times 10^6 (d_m T)^{1.5}}{W_m}]^{1/2} \quad (13)$$

where

V_s = Strike velocity of the missile (ft/sec)

d_m = Diameter (or equivalent diameter) of the missile (in.)

T = Thickness of the steel plate (in.)

W_m = Weight of the missile (lbs)

Eqn. 13 may be used for estimating the residual velocity of a missile after it has perforated a target. For example, suppose an existing door is not capable of stopping a certain missile. Eqn. 13 could be used to estimate the velocity of the missile after it passes through the door.

2. Structural Response to Missile Impact

When a missile strikes a structural component such as a beam or slab, the failure mechanism may be due to overall structural response rather than penetration. Of the missiles specified in Table V, only the automobile is likely to cause this type of response.

Missile impact may be either elastic or plastic. In the case of elastic impact the missile and target remain in contact for a very short time and then disengage because of elastic interface restoring forces. Plastic impact is characterized by the missile remaining in contact with the target subsequent to impact. Recent impact tests (Stephenson 1975) indicate that both the timber missiles and the automobile result in plastic impact when they strike a solid object such as a concrete wall. For this reason only the plastic impact case is treated in this report.

Several methods are available for estimating the maximum response. The Energy Balance method uses the strain energy of the target at

maximum response to balance the residual kinetic energy of the target (or target-missile combination) resulting from missile impact. An alternative approach, referred to as the Acceleration Pulse Method, is possible, if the target-missile interface loading function is known, and if the dynamic system is modeled as a one degree-of-freedom elasto-plastic system. This latter method is recommended for studying the impact effects of the automobile. The maximum response predicted by the Energy Balance method is 2 to 3 times greater than that predicted by the acceleration-pulse technique. However, the latter values are considered to be more realistic even though they are lower.

In experiments with automobile crashes an approximate force-time function for frontal impact has been derived (Bechtel 1973).

$$F(t) = 0.625 V_s W_m \sin 20.06t \quad (14)$$

where

V_s = missile (automobile) strike velocity (ft/sec)

W_m = weight of automobile (lbs)

The function is a sine wave with frequency $\omega = 20.06$ rad/sec and period

$$\begin{aligned} T &= 2\pi/\omega \\ &= 0.314 \text{ sec.} \end{aligned} \quad (15)$$

The maximum force occurs at $t = \bar{T}/4 = 0.0785$ sec. Under the condition of plastic impact (i.e. target and missile acquire the same velocity

after impact) the duration of the impact force is from $t = 0$ to $t = 0.785$ sec. At $t = 0.0785$ sec the interface force diminishes to zero.

The maximum target response is obtained by writing the equation of motion for a one-degree-of-freedom elasto-plastic oscillator with damping neglected.

$$M' \ddot{y} + R(y) - F(t) = 0 \quad (16)$$

In this equation

M' = effective mass of the target plus the mass of the missile ($lb \cdot sec^2/ft$)

$R(y)$ = resistance function for the target material (lb)

$F(t)$ = target-automobile interface force function (lb)

For elasto-plastic target response with no other concurrent loads on the target, the resistance function is

$$R(y) = Ky \quad (0 < y < y_{el})$$

$$R(y) = Ky_{el} = R_m \quad (y_{el} < y < y_{max}) \quad (17)$$

where

y = the displacement of the target (ft)

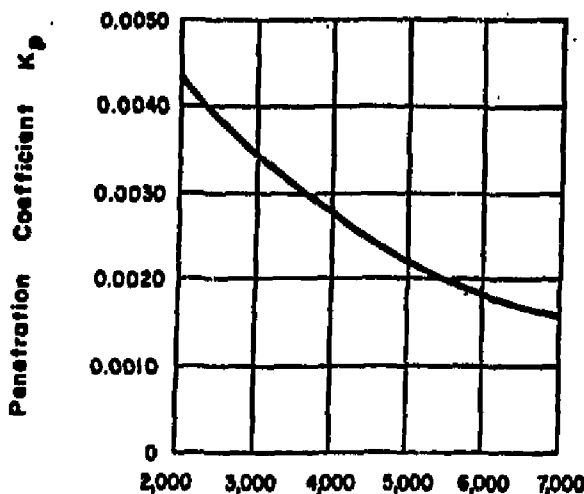
y_{el} = the displacement at yield in the target material (ft)

K = stiffness of the target (lb/ft)

R_m = maximum plastic resistance

The above relationships are illustrated in Fig. 5.

The effective target mass during impact varies and generally increases to a maximum at the end of the impact duration. Expressions



28 - Day Compressive Strength of Concrete

FIGURE 4. VALUES OF PENETRATION COEFFICIENT K_p FOR REINFORCED CONCRETE

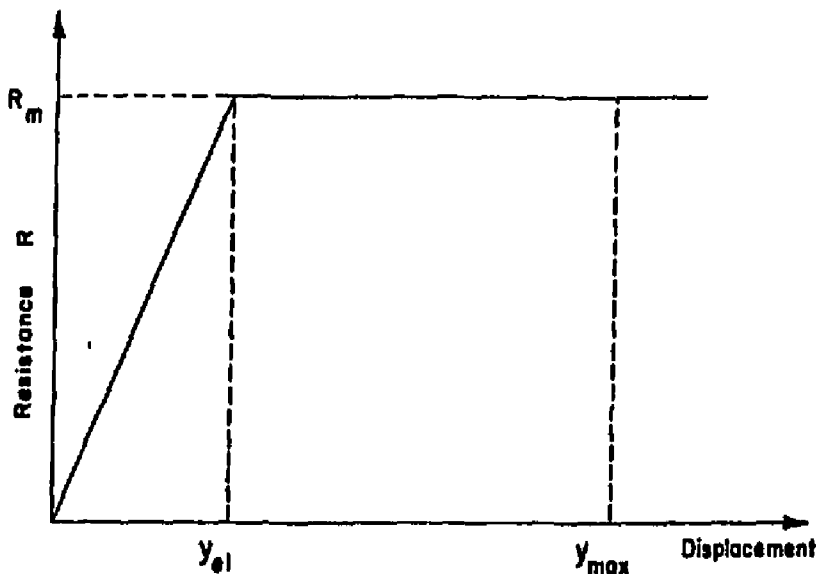


FIGURE 5. IDEALIZED RESISTANCE-DISPLACEMENT FUNCTION FOR DUCTILE MATERIALS

for estimating the average effective mass are given in Table VII.

The equation of motion may be solved by numerical techniques. The problem may be further simplified by replacing the load function given by Eqn. 14 with an equivalent rectangular pulse. The applied impulse is, by definition, the area under the load function. Integrating over the load duration

$$\begin{aligned} I &= \int (0.625 V_s W_m \sin 20.06t) dt \\ &= 0.625 V_s W_m \left[\frac{-1}{20.06} \cos 20.06t \right]_0^{0.0785} \\ &= 0.625 V_s W_m (0.05) \end{aligned} \quad (18)$$

Thus an equivalent rectangular pulse is one whose magnitude is

$F_1 = 0.625 V_s W_m$ and whose time duration is $t_d = 0.05$ sec.

The Acceleration-Pulse method of numerical integration gives a reasonable solution if the time step Δt is taken less than one tenth the fundamental period of the target. The displacement during the first time step is estimated using the equation

$$y_1 = \frac{1}{2} \ddot{y}_0 (\Delta t)^2 \quad (19)$$

Displacements in subsequent time steps are obtained from the recurrence relationship

$$y_{t+1} = 2y_t - y_{t-1} + \ddot{y}_t (\Delta t)^2 \quad (20)$$

Once the maximum displacement has been found, the ductility ratio u is calculated

$$u = \frac{y_{\max}}{y_{el}} \quad (21)$$

TABLE VII
EFFECTIVE MASS OF TARGET
DURING IMPACT

Concrete Beams:

$$M_e = (D_x + 2T) \frac{BT\gamma_c}{g} \quad (B < D_y + 2T)$$

$$M_e = (D_x + 2T) (D_y + 2T) T \frac{\gamma_c}{g} \quad (B > D_y + 2T)$$

Concrete Slabs:

$$M_e = (D_x + T)(D_y + T) T \frac{\gamma_c}{g}$$

Steel Beams:

$$M_e = (D_x + 2D) M_x$$

Steel Plates:

$$M_e = D_x D_y T \frac{\gamma_s}{g}$$

D_x = Maximum missile contact dimension in the x-direction (longitudinal direction for beams and slabs)

D_y = Maximum missile contact dimension in the y-direction (transverse to longitudinal direction for beams and slabs)

B = Width of concrete beam (not to exceed $D_y + 2T$)

T = Depth of concrete beam or thickness of concrete slab

γ_x = Mass per unit length of steel beam

γ_c = Unit weight of concrete

γ_s = Unit weight of steel

g = Acceleration due to gravity

The maximum recommended ductility ratios to absorb energy of missile impact for various components are given in Table VIII. The ratios should be reduced appropriately if axial loads in addition to lateral impact loads are involved. For reinforced concrete walls, the ductility ratios given in the Table are for low percentage of reinforcement; the ratios should be reduced if higher than recommended percentage of reinforcement is used. Precautions should be taken to prevent premature failure of reinforced concrete wall slab due to diagonal tension, due to punching shear, or due to bond failure. If reinforcing bars are terminated in the tension zone in the wall slab, there could be a reduction in the capacity of the slab. In the case of steel beams the flanges must be thick enough to prevent local buckling.

The Acceleration-Pulse technique is illustrated in an example problem in Section III. D. 5. c.

TABLE VIII
RECOMMENDED DUCTILITY RATIOS

<u>Component</u>	<u>Maximum Ductility Ratio</u>
Steel Beam	15
Concrete Beam or One-Way Slab	10 (with $\rho^* \leq 0.01$)
Concrete Two-Way Wall Slab	20 (with $\rho \leq 0.005$ in each direction)

$\rho^* = \frac{A_s}{bd}$; ratio of steel area to concrete area.

D. Design Example

This example treats the case of reinforced concrete building that might be found at Site 300. The example is not modeled after any particular building at the site. Only the design loads are determined. Structural design of the individual components of the building is beyond the scope of these guidelines.

A plan view of the building outline is shown in Fig. 6. Overall dimensions of the building are 92 ft x 24 ft. The wall height is 30 ft in the critical area. The critical nature of functions performed inside the building requires that the structural integrity of the building be maintained. All doors and openings shall be designed to withstand the pressures resulting from the design windspeeds and the impacts from windborne missiles.

1. Design Criteria

The critical portions of the building shall withstand wind loadings equivalent to:

Maximum windspeed, 203 mph

Missiles: Timber with nominal dimensions 4 in. x 12 in. x 12 ft long weighing 139 lbs and traveling at 90 mph (horizontal) and 60 mph (vertical).

Automobile weighing 4000 lbs tumbling at 25 mph.

2. Wind Induced Loads

The effective velocity pressure is $q = 106 \text{ psf}$. Since the wall height is less than or equal to 30 ft, no adjustment in q is needed because of height.

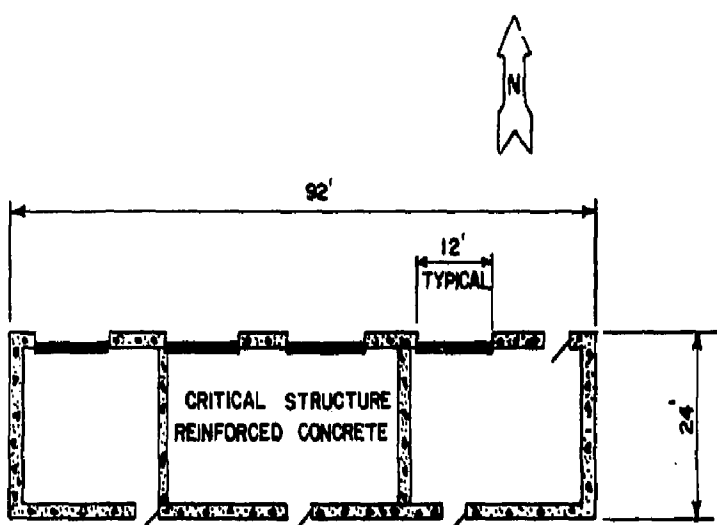


FIGURE 6. PLAN VIEW OF EXAMPLE STRUCTURE

a. External Pressure

From ANSI A58.1, Table 7:

$$\text{Windward wall: } (+0.8)(106) = 85 \text{ psf}$$

$$\text{Leeward wall: } (-0.5)(106) = -53 \text{ psf}$$

$$\text{Side wall: } (-0.7)(106) = -74 \text{ psf}$$

$$\text{Roof: } (-0.7)(106) = -74 \text{ psf}$$

b. Local Effects

Wall corners: $(-2.0)(106) = -212 \text{ psf}$ acting on a strip 2.4 ft wide at outside corner.

Eaves (all around perimeter of roof):
 $(-2.4)(106) = -254 \text{ psf}$ acting on a strip 2.4 ft wide.

Roof corners: $(-5.0)(106) = -530 \text{ psf}$ acting on an area 2.4 ft x 2.4 ft at all corners.

3. Wind Induced Roof Diaphragm and Shear Wall Loads

The walls are assumed simply supported at the footing and at the roof.

a. Winds from North or South

$$\text{Diaphragm load: } (106)(+0.8 + 0.5)(30)/2 = 2067 \text{ plf}$$

$$\text{Total diaphragm load} = 2067(92)$$

$$= 190,200 \text{ lb}$$

$$\text{Force per ft on shear walls} = \frac{190,200}{2 \times 24} \\ = 3962 \text{ plf}$$

b. Winds from East or West

$$\text{Diaphragm load} = 106(0.8 + 0.5)(30)/2$$

$$= 2067 \text{ plf}$$

Total diaphragm load = 2067(24)
= 49,610 lb

Force per ft on shear wall = $\frac{49,610}{2} (1/32)$
= 270 plf

4. Controlling Design Wind Loads

a. Walls

1. +85 psf (acting inward)
2. -74 psf (acting outward)
3. -212 psf acting outward on a strip 2.4 wide at each outside corner. This load primarily controls the horizontal steel required to tie the two intersecting walls together. It is not used in combination with other externally applied loads.
4. 3962 plf load on shear walls at east and west end of the building.
5. 270 plf load on shear walls at north and south sides of the building.

b. Roof

1. -74 psf acting upward.
2. -254 psf acting on 2.4 ft wide strip all around the perimeter of the building. This load controls the steel required to anchor the roof slab to the top of the walls. It should not be used in combination with any other loads.
3. -530 psf acting upward on a 2.4 ft x 2.4 ft area at each roof corner. This load also affects the anchorage of the roof slab to the top of the walls. It should not be used in combination with any other loads.

c. Components

1. +85 psf
2. -74 psf
3. Local effects (at wall corners, roof corners and eaves), if the component is located within the areas influenced by the local effects.

5. Missile Induced Loads

Three examples are presented below which illustrate the use of the missile penetration formulas:

a. Reinforced Concrete Target

The Modified Petry Formula should be used to determine the thickness of reinforced concrete required to resist the design timber missile.

Assume $f'_c = 4000$ psi for the concrete.

Determine the minimum thickness of the wall to just prevent perforation:

The Modified Petry Formula is given by Eqn. 9.

$$K_p = 0.0028 \text{ for } f'_c = 4000 \text{ psi (Ref. Figure 4)}$$

$$A_p = \frac{139}{41.77144} = 480 \text{ psf}$$

$$V_s = 90 \text{ mph} = 132 \text{ fps}$$

$$D = 12(0.0028)(480) \log_{10} \left[1 + \frac{(132)^2}{215,000} \right]$$

$$= 0.55 \text{ in.}$$

Clearly, missile penetration into a reinforced concrete wall is not critical for this design windspeed.

b. Steel Target:

Determine the thickness of a steel plate in an overhead door to prevent penetration of the design missile:

Neglect deflection of the door and assume the supports are rigid.

$$M_m = \frac{139}{32.2} = 4.32 \text{ slugs}$$

$$V_s = 132 \text{ fps}$$

$$A = \text{Area of missile} = 41.7 \text{ in.}^2$$

The equivalent circular diameter is

$$d_m = \sqrt{\frac{4A}{\pi}} \quad (17)$$

$$= \sqrt{\frac{4(41.7)}{\pi}} = 7.29 \text{ in.}$$

The thickness of the plate to just prevent perforation is obtained from the BRL formula

$$T = \frac{\left[\frac{4.32(132)^2}{672(7.29)} \right]^{2/3}}{2} = 0.23 \text{ in. (Equation 11)}$$

The design thickness should be

$$T_p = 1.25T \\ = 0.29 \text{ in. (Equation 12)}$$

Suppose the material available for the door cladding is only 1/8 in. thick. Estimate the residual velocity of the design missile after perforation. Use Eqn. 13:

$$V_r = \left[(132)^2 - 1.12 \times 10^6 \frac{(7.29 \times 0.125)^{1.5}}{139} \right]^{1/2} \\ = 102 \text{ ft/sec (70 mph)}$$

c. Structural Response of a Concrete Wall to the Impact of a Tumbling Automobile

Check the adequacy of a 12 in. concrete wall panel when impacted by a 4000 lb automobile ($M = 124.3$ slugs) traveling at 25 mph (36.7 ft/sec). The wall is simply supported at top and bottom and has a height of 15 ft. The point of impact is 5 ft above the base of the wall as shown in Fig. 7.

Assume:

$$f_c' = 3000 \text{ psi}$$

$$f_s = 40,000 \text{ psi}$$

Vertical steel #9 @ 12" o.c.

$$A_s = 0.99 \text{ in.}^2/\text{ft of wall}$$

Calculate wall parameters (Refer to Fig. 8):

$$d = 12 - 1.31 = 10.69 \text{ in.}$$

$$\rho = \frac{0.99}{10.69(12)} = 0.00772$$

A value of $\rho < 0.5 \rho_b$ assures adequate ductility of the slab.

$$n = \frac{29 \times 10^6}{(150)^{1.5} (33) \sqrt{3000}} = 8.73$$

Use $n = 9$

Calculate the yield moment M_y on the basis of straight line theory:

$$12(kd) \frac{kd}{2} = 8.91 (10.69 - kd) \quad (22)$$

$$kd = 3.25 \text{ in.}$$

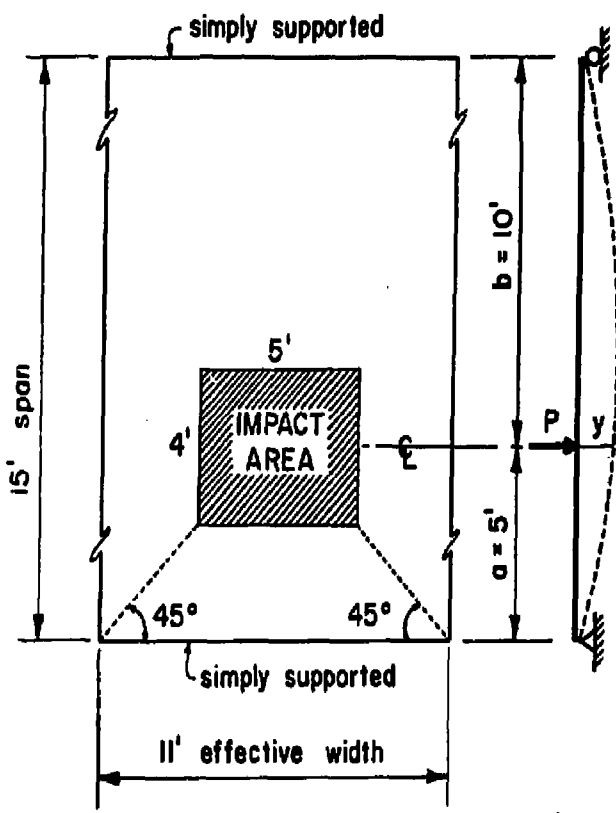


FIGURE 7. STRUCTURAL RESPONSE OF A REINFORCED CONCRETE WALL

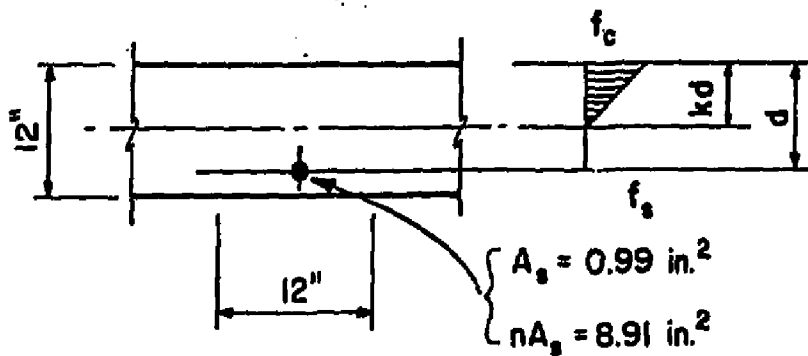


FIGURE 8. REINFORCED CONCRETE WALL
CROSS SECTION

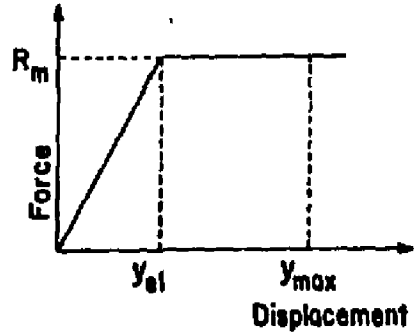
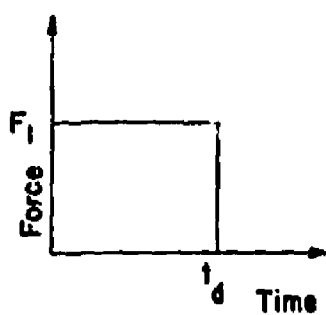


FIGURE 9. FORCE-TIME FUNCTION AND
RESISTANCE FUNCTION

$$\begin{aligned}
 M_y &= f_s A_s j d \\
 &= 40,000 (0.99) (10.69 - \frac{3.25}{3}) \\
 &= 380,400 \text{ in. lb/ft} \\
 &= 3.49 \times 10^5 \text{ ft. lb/(11 ft width)}
 \end{aligned}$$

Check f_c :

$$\begin{aligned}
 C &= 40,000 (0.99) \\
 &= 39,600 \text{ lb}
 \end{aligned}$$

$$\begin{aligned}
 f_c &= 2C/bkd \quad (24) \\
 &= \frac{2(39,600)}{12(3.25)} \\
 &= 2031 \text{ psi} < 0.7f'_c
 \end{aligned}$$

Note that for this cross section

$$M_u = 397,800 \text{ in. lb/ft}$$

$$M_y = 0.96 M_u$$

Calculate moment of inertia

$$\begin{aligned}
 I_0 &= \frac{12 (3.25)^3}{3} + 8.91 (10.69 - 3.25)^2 \\
 &= 630.5 \text{ in}^4/\text{ft} \\
 &= 6936 \text{ in}^4/(11 \text{ ft width})
 \end{aligned}$$

Stiffness of one way slab

$$K = \frac{3EI}{a^2 b^2}$$

$$\begin{aligned}
 &= \frac{3(3.2 \times 10^6)(6936)(15)}{(5)^2 (10)^2 (144)} \\
 &= 2.77 \times 10^5 \text{ lb/ft} / (11 \text{ ft width})
 \end{aligned} \tag{25}$$

The maximum resistance of the slab is

$$\begin{aligned}
 R_m &= \frac{M_y L}{ab} \\
 R_m &= \frac{3.49 \times 10^5 (15)}{(5) (10)} \\
 R_m &= 1.05 \times 10^5 \text{ lb}
 \end{aligned} \tag{26}$$

The deflection to produce yield is

$$\begin{aligned}
 y_{el} &= \frac{R_m}{K} \\
 &= \frac{1.05 \times 10^5}{2.77 \times 10^6} \\
 &= 0.0378 \text{ ft} \quad (0.45 \text{ in.})
 \end{aligned} \tag{27}$$

For the impact of an automobile the loading is considered to be a rectangular load pulse. The magnitude of the pulse is

$$F_1 \approx 0.625 V_s W_m \tag{28}$$

where V_s = strike velocity of the automobile (ft/sec)

W_m = weight of the automobile (lbs)

In this example

$$F_1 \approx 0.625 (36.7)(4000)$$

$$\approx 9.18 \times 10^4 \text{ lb}$$

The duration of the load pulse t_d is 0.05 sec. The load pulse and assumed resistance function are shown in Fig. 9.

The impact is assumed to be plastic. Thus upon impact the velocity of the wall and the automobile are the same and they move together to the point of maximum deflection, y_{max} . The equivalent mass of the slab itself is (Table VII):

$$M_e = (D_x + T)(D_y + T)(T) \frac{\gamma_c}{g} \quad (29)$$

where D_x, D_y = dimensions of the contact area (ft)

γ_c = the unit weight of concrete (lb/ft³)

g = acceleration due to gravity (ft/sec²)

T = the thickness of the concrete (ft)

$$M_e = 6(5)(1)(150)/32.2$$

$$= 139.8 \text{ lb.sec}^2/\text{ft}$$

Since the effective mass of the target and the missile move together the total mass is

$$\begin{aligned} M^* &= M_e + M_m \\ &= 139.8 + 124.2 \\ &= 264.0 \text{ lb.sec}^2/\text{ft} \end{aligned} \quad (30)$$

The equation of motion in general terms for this one-degree-of-freedom elasto-plastic system is

$$M^*y'' + R(y) - F(t) = 0 \quad (\text{Equation 16})$$

Or, because of the nature of the assumed resistance function

$$\begin{aligned} M\ddot{y} + Ky - F_1 &= 0 & (0 < y < y_{el}) \\ M\ddot{y} + R_m - F_1 &= 0 & (y_{el} < y < y_{max}) \end{aligned} \quad (31)$$

Substituting appropriate values and rearranging, the equations become

$$\begin{aligned} \ddot{y} &= 347.7 - 1.049 \times 10^4 y & (0 < y < 0.0378) \\ \ddot{y} &= 347.7 - 397.7 \\ &= -50.0 & (0.0378 < y < y_{max}) \end{aligned} \quad (32)$$

The above equations may be solved by using numerical integration, or the tables and charts in Biggs (1964) can be used to determine y_{max} and the time t_{max} at which it occurs.

The Acceleration-Pulse method is presented in this example. The relationship needed to determine the displacement during the first time step is

$$y_1 = 1/2 \ddot{y}_0 (\Delta t)^2 \quad (\text{Equation 19})$$

Subsequent displacements are given by the recursion formula

$$y_{t+1} = 2y_t - y_{t-1} + \ddot{y}_t (\Delta t)^2 \quad (\text{Equation 20})$$

The period for this equivalent one-degree-of-freedom system is given by

$$\begin{aligned} \bar{t} &= 2\pi \sqrt{\frac{M}{K}} \\ &= 2\pi \sqrt{\frac{264.0}{2.77 \times 10^6}} \\ &\approx 0.061 \text{ sec} \end{aligned} \quad (33)$$

The time step Δt should be less than $\bar{t}/10$. Use $\Delta t \leq 0.006$ sec. The calculations are summarized in Table IX. The maximum deflection ($y_{\max} = 0.127$ ft) occurs at $t = 0.054$ sec. The corresponding ductility ratio is

$$u = \frac{y_{\max}}{y_{el}} = \frac{0.127}{0.0378} = 3.36 \quad (\text{Equation 21})$$

The ductility ratio is well within the allowable of 10 recommended in Table VIII. Therefore the 12 in. concrete slab is adequate to resist the impact of the 4000 lb automobile traveling at 25 mph.

Note that the wall height used in the calculation of the structural response was not 30 ft as given in the example problem. A 30 ft high wall impacted 5 ft from its support is more likely to experience a shear response failure rather than due to bending. Therefore the 15 ft high wall was used in the example to illustrate the Acceleration Pulse method as outlined in Section C. 2.

TABLE IX
NUMERICAL SOLUTION TO EQUATIONS OF MOTION

Time Step	Elapsed Time Sec	F_1/M ft/sec^2	R/M ft/sec^2	\ddot{y} ft/sec^2	$\ddot{y} \Delta t^2$ ft	y ft
0	0	347.7	0	347.7	1.39×10^{-3}	0
1	.002		-7.29	340.4	1.36×10^{-3}	6.95×10^{-3}
2	.004		-28.89	318.8	1.28×10^{-3}	2.75×10^{-3}
3	.006		-63.83	283.9	1.14×10^{-3}	6.08×10^{-3}
4	.008		-111.0	237	9.48×10^{-4}	1.06×10^{-2}
5	.010		-168	180	7.21×10^{-4}	1.60×10^{-2}
6	.012		-232	116	4.63×10^{-4}	2.21×10^{-2}
7	.014		-301	47	1.86×10^{-4}	2.87×10^{-2}
8	.016		-372	-25	-9.84×10^{-5}	3.55×10^{-2}
9	.018		397.7	-50	-2.0×10^{-4}	4.22×10^{-2}
10	.020					4.87×10^{-2}
11	.022					5.50×10^{-2}
12	.024					6.10×10^{-2}
13	.026					6.69×10^{-2}
14	.028					7.26×10^{-2}
15	.030					7.81×10^{-2}
16	.032					8.34×10^{-2}
17	.034					8.85×10^{-2}
18	.036					9.34×10^{-2}
19	.038					9.81×10^{-2}
20	.040					1.03×10^{-1}
21	.042					1.07×10^{-1}
22	.044					1.11×10^{-1}
23	.046					1.15×10^{-1}
24	.048					1.18×10^{-1}
25	.050	347.7	397.7	-50	-2.0×10^{-4}	1.22×10^{-1}

TABLE IX (CONT'D)
NUMERICAL SOLUTION TO EQUATIONS OF MOTION

Time Step	Elapsed Time Sec	F_1/M ft/sec ²	R/M ft/sec ²	\ddot{y} ft/sec ²	$\ddot{y} \Delta t^2$ ft	y ft
26	.052	0	397.7	-397.7	-1.59×10^{-3}	1.25×10^{-1}
27	.054	0	397.7	-397.7	-1.59×10^{-3}	1.27×10^{-1}
28	.056	0	397.7	-397.7	-1.59×10^{-3}	1.27×10^{-1}
29	.058	0				1.26×10^{-1}

APPENDIX A

TABLE OF FUJITA-PEARSON TORNADO SCALE. Characteristics of a tornado can be expressed as a combination of Fujita-scale windspeed and Pearson-scale path length and width. This scale permits us to classify tornadoes between two extreme FPP scales, 0,0,0 and 5,5,5.

F-scale Maximum Windspeed				F-scale Path Length			F-scale Path Width			
Scale	mph	kts	m/s	Scale	miles	km	Scale	ft	yds	meters
F 0.0	40	35	18	F 0.0	0.3	0.5	F 0.0	17	6	5
0.1	43	37	19		0.1	0.6		19	6	6
0.2	46	40	21		0.2	0.6		21	7	6
0.3	49	43	22		0.3	0.7		24	8	7
0.4	52	46	23		0.4	0.8		26	9	8
0.5	56	48	25		0.5	0.9		30	10	9
0.6	59	51	26		0.6	1.0		33	11	10
0.7	63	54	28		0.7	1.1		37	13	11
0.8	66	57	30		0.8	1.3		42	14	13
0.9	70	60	31		0.9	1.4		47	16	14
F 1.0	73	64	33	F 1.0	1.0	1.6	F 1.0	53	18	16
1.1	77	67	34		1.1	1.8		59	20	18
1.2	81	70	36		1.2	2.0		66	22	20
1.3	84	73	38		1.3	2.3		74	25	23
1.4	88	77	40		1.4	2.6		84	28	26
1.5	92	80	41		1.5	2.9		94	31	29
1.6	96	84	43		1.6	3.2		105	35	32
1.7	100	87	45		1.7	3.6		118	39	36
1.8	104	91	47		1.8	4.0		133	44	40
1.9	109	94	49		1.9	4.5		149	50	45
F 2.0	113	98	50	F 2.0	3.2	5.1	F 2.0	167	56	51
2.1	117	102	52		2.1	5.5		187	62	57
2.2	121	105	54		2.2	6.4		210	70	64
2.3	126	109	56		2.3	7.2		235	78	72
2.4	130	113	58		2.4	8.1		265	88	81
2.5	135	117	60		2.5	9.0		297	99	90
2.6	139	121	61		2.6	10.3		333	111	103
2.7	144	125	64		2.7	11.4		374	125	114
2.8	148	129	66		2.8	12.8		419	140	128
2.9	153	132	68		2.9	14.3		470	157	143
F 3.0	158	137	70	F 3.0	10.0	16.1	F 3.0	528	176	161
3.1	162	141	73		3.1	18.0		591	197	180
3.2	167	145	75		3.2	20.3		665	222	203
3.3	172	149	77		3.3	22.7		744	248	227
3.4	177	154	79		3.4	25.6		837	279	256
3.5	182	158	81		3.5	28.6		940	313	286
3.6	187	162	83		3.6	32.2		1054	351	322
3.7	192	167	86		3.7	36.0		1183	394	360
3.8	197	171	88		3.8	40.4		1326	442	404
3.9	202	175	90		3.9	45.4		1489	496	454
F 4.0	207	180	93	F 4.0	31.6	50.9	F 4.0	1670	557	509
4.1	212	184	95		4.1	55.5		1874	625	571
4.2	218	189	97		4.2	64.1		2102	701	641
4.3	223	194	100		4.3	71.6		2354	785	718
4.4	228	198	102		4.4	80.6		2646	882	806
4.5	233	203	104		4.5	90.4		2967	989	904
4.6	238	207	107		4.6	102		3332	1111	1000 km
4.7	244	212	109		4.7	114		3738	1246	111
4.8	250	217	112		4.8	128		4194	1398	123
4.9	255	222	114		4.9	143		4704	1568	144
F 5.0	261	227	117	F 5.0	100	161	F 5.0	1.0 mi	1760	1.6
5.1	267	232	119		5.1	181		1971	1.8	
5.2	273	236	122		5.2	203		2218	2.0	
5.3	278	241	124		5.3	227		2482	2.3	
5.4	284	246	127		5.4	255		2798	2.6	
5.5	289	251	129		5.5	286		3133	2.9	
5.6	295	256	132		5.6	321		3520	3.2	
5.7	301	261	135		5.7	360		3942	3.6	
5.8	307	267	137		5.8	404		4418	4.0	
5.9	313	272	140		5.9	454		4963	4.5	

APPENDIX B

Windspeed Probabilities Based on Fisher-Tippett Type II Distribution

For more specific details of the calculations presented herein, reference is made to Thom (1968). The Fisher-Tippett Type II distribution is given by the equation

$$F(V) = \exp [-(V/\beta)^{-\gamma}] \quad (B1)$$

where:

$F(V)$ is the probability that the windspeed will not exceed the value V in one year

β, γ are constants to be determined.

Values of β and γ are determined for a specific location from the data presented in the Thom article. Contour maps are presented for annual extreme-mile windspeeds for 2, 10, 25, 50 and 100 year mean recurrence intervals. These values are plotted on the special Fisher-Tippett Type II probability paper (Figure B1) and a best fit straight line is drawn through the points. In this case only the lower four points were used as explained in Section IID. Then by observing from the curve that

$$F(32) = 0.010$$

$$F(84) = 0.999,$$

Equation (B1) may be used to solve for γ and β .

$$0.010 = \exp [-(32/\beta)^{-\gamma}]$$

$$0.999 = \exp [-(84/\beta)^{-\gamma}]$$

Values are found to be

$$\beta = 38.43$$

$$\gamma = 8.78$$

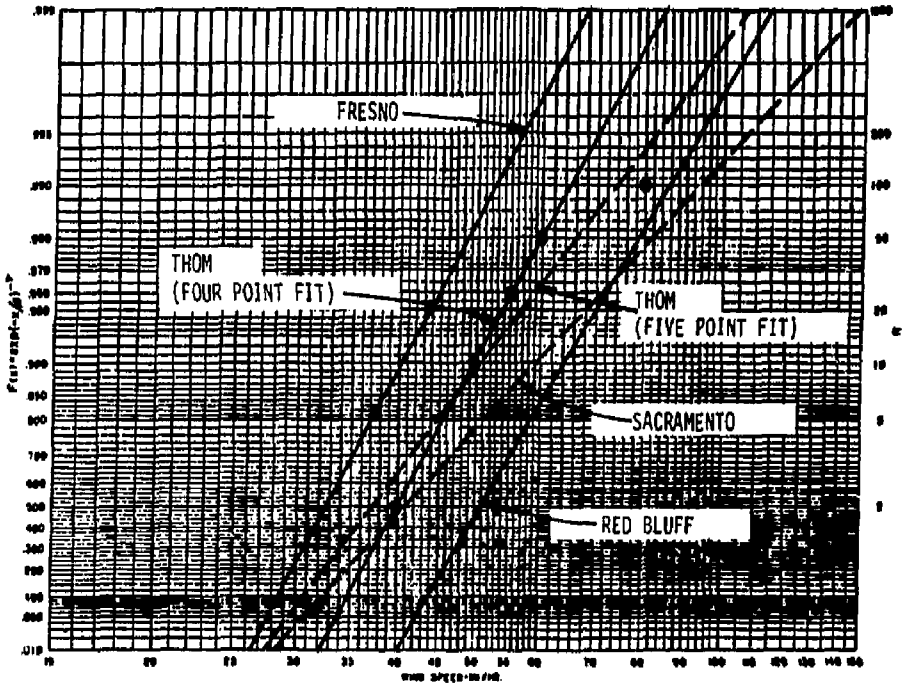
Equation (B1) thus becomes

$$F(V) = \exp [-(V/38.43)^{-8.78}] \quad (B2)$$

where V is expressed in mph.

The probability that the windspeed will exceed a value V is

$$P_E = 1 - F(V) \quad (B3)$$



MAXIMUM-VALUE PROBABILITY PAPER, FISHER-TIPPETT TYPE II DISTRIBUTION.

FIGURE B1. FISHER-TIPPETT TYPE II PROBABILITY FOR SITE 300

LIST OF REFERENCES

AEC, 1974: Design Basis Tornado for Nuclear Power Plants, Regulatory Guide 1.76, April 1974.

ANSI, 1972: American National Standard: Building Code Requirements for Minimum Design Loads in Buildings and Other Structures, ANSI A58.1-1972, ANSI, New York, 60 pp.

Bechtel Power Corporation, "Design of Structures for Missile Impact," BC-TOP-9, Revision 1, Bechtel Power Corporation, San Francisco, California, July 1973.

Biggs, J. M., Introduction to Structural Dynamics, McGraw-Hill Book Company, New York, 1964.

Brenner, I. S., 1974: A Surge of Maritime Tropical Air-Gulf of California to the Southwestern United States. Mon. Wea. Rev., 102, 375-389.

Court, A., 1970: Tornado Incidence Maps. ESSA Tech. Memo. ERLTM-NSSL 49, 76 pp.

Critchfield, H. J., 1960: General Climatology, Englewood Cliffs, N. J. (Prentice-Hall), 465 pp.

Day, P. C., 1930: Weather Bureau gets Data on Behavior and Effects of Tornadoes, Yearbook of Agriculture, U. S. Dept. of Agriculture, 530-534.

Dodd, A. V., "A Real Distribution and Diurnal Variation of Water Vapor Near Ground in the Contiguous United States", Technical Report ES-17, Earth Sciences Division, W. S. Material Command, U. S. Army Natick Laboratories, Natick, Mass., Nov. 1965.

Feris, C., 1970: The Tornado at Kent, Washington. Weatherwise, 23, 75-77, 83.

Finley, J. P., 1884: Report on the Character of 600 Tornadoes. Pap. Signal Serv., No. 7, 29 pp.

Flora, S. D., 1953: Tornadoes of the United States. University of Oklahoma Press, Norman, 271 pp.

Fujita, T. T., 1970: Estimate of Maximum Windspeeds of Tornadoes in Three Northwestern States. SMRP Rpt. No. 72, University of Chicago, 27 pp.

_____, 1971: Proposed Characterization of Tornadoes and Hurricanes by Area and Intensity. SMRP Rpt. No. 91, University of Chicago, 42 pp.

_____, 1972: Estimate of Maximum Windspeeds of Tornadoes in Southernmost Rockies. SMRP Rpt. No. 105, University of Chicago, 47 pp.

_____, 1973: Tornadoes Around the World. Weatherwise, 26, 56-62, 78-83.

Hales, J. E., Jr., 1974: Southwestern United States Summer Monsoon Source -- Gulf of Mexico or Pacific Ocean? J. Appl. Meteor., 13, 331-342.

Hoecker, W. H., Jr., "Wind Speed and Air Flow Patterns in the Dallas Tornado of April 2, 1957," Monthly Weather Review, Vol. 88, No. 5, pp. 167-180, 1960.

McDonald, J. R., 1974: Tornado Risks and Design Windspeeds for the Oak Ridge Plant Site. Institute for Disaster Research, Texas Tech University, Lubbock, Texas, 23 pp.

_____, 1974a: Tornado Risks and Design Windspeeds for the Portsmouth Plant Site. Institute for Disaster Research, Texas Tech University, Lubbock, Texas, 23 pp.

Kessler, Edwin, 1974: "Survey of Boundary Layer Winds with Special Response to Extreme Values," American Institute of Aeronautics and Astronautics, Paper No. 74-586.

Miller, R. C., 1970: Notes on Analysis and Severe-Storm Forecasting Procedures of the Air Force Global Weather Central. TR200 (Rev), AWS USAF.

Neville, A. M. and Kennedy, J. B., Basic Statistical Methods for Engineers and Scientists, International Textbook Company, Scranton, PA, 1966.

NOAA: Storm Data, Monthly Weather Summary by NOAA Environmental Data Service, Asheville, North Carolina (Published since 1956).

NSSFC, 1974: Computer Records of Tornado Occurrences. National Weather Service, Kansas City.

Pautz, M. E., ed., 1969: Severe Local Storm Occurrences, 1955-1967, ESSA Tech. Memo. WBTM FCST 12, U. S. Weather Bureau, 77 pp.

Rasmussen, E. M., 1967: Atmospheric Water Vapor Transport and the Water Balance of North America. Pt. 1. Mon. Wea. Rev., 95, 403-426.

Showalter, A. K. and J. R. Fulks, 1943: Preliminary Report on
Tornadoes, U. S. Weather Bureau, 163 pp.

Smith, T. B. and V. A. Mirabella, 1972: Characteristics of California
Tornadoes, Final Rpt., MRI 72 FT-996, 25 pp.

Thom, H. C. S., 1968: New Distributions of Extreme Winds in the
United States, Proc. Structural Div. ASCE, 94, ST7.

Trewartha, G. T., 1961: The Earth's Problem Climates, Madison
(Univ. of Wisconsin), 334 pp.

U. S. Department of Commerce, "Climatic Atlas of the United States,"
Environmental Data Service ESSA, June 1968.

DISTRIBUTION

Bob Murray	105
TID, File	3
TIC, Oak Ridge, TN	2

NOTICE

"This report was prepared as an account of work sponsored by the United States Government. Neither the United States nor the United States Energy Research & Development Administration, nor any of their employees, nor any of their contractors, subcontractors, or their employees, makes any warranty, express or implied, or assumes any legal liability or responsibility for the accuracy, completeness, or usefulness of any information, apparatus, product or process disclosed, or represents that its use would not infringe privately-owned rights."